Solar Energy Materials 1 (1979) 11-27
©North-Holland Publishing Company

OPTICAL PROPERTIES AND STRUCTURE OF AMORPHOUS SILICON FILMS PREPARED BY CVD*

M. JANAI**, D. D. ALLRED, D. C. BOOTH and B. O. SERAPHIN
Optical Sciences Center, University of Arizona, Tucson, AZ 85721, USA

Received in revised form 25 May 1978

Silicon films were deposited by pyrolytic decomposition of silane on substrates held at various temperatures, T_s, in the range 550 to 800°C. The absorption coefficient, refractive index, and X-ray diffraction pattern of these films were determined. The films deposited at temperatures $T_s \leq 660$°C are amorphous, and their absorption profile resembles that reported in the literature for sputtered or evaporated amorphous films after long-time anneal. Films deposited on substrates at or above 670°C are partially crystallized, with particle size increasing gradually with substrate temperature. When the amorphous films are annealed, the resulting changes depend on length and temperature of the anneal. After a temperature-dependent induction period, the samples crystallize rapidly. The volume shrinks by $\approx 3\%$, as determined from the decrease in film thickness. The onset of crystallization is indicated first by a red shift of the absorption edge, which after further anneal is overcompensated by a blue shift. The results demonstrate that the superior solar absorptance of amorphous silicon can be utilized in photothermal solar energy converters of sufficient stability without sacrificing the advantages of CVD fabrication.

1. Introduction

The optical properties and the structure of amorphous silicon films and other tetrahedrally bonded amorphous semiconductors have been the subject of numerous investigations in recent years (Theye [1]). These investigations have found that both the structure and the optical properties of the amorphous film depend drastically on the preparation conditions and the thermal history of the samples. The methods of preparation most commonly studied are vacuum evaporation, sputtering, and glow-discharge decomposition of silane. Preparation of amorphous silicon films by chemical vapor deposition (CVD), or pyrolytic decomposition as it is sometimes called (Kamins [2]), has received less attention, probably because the pyrolytic decomposition of silane is commonly performed in a temperature range that results in a polycrystalline film. Nevertheless, it is mentioned several times in the literature that at deposition temperatures below 650 to 700°C the pyrolytic decomposition of silane results in an amorphous film, as indicated by electron or X-ray diffraction patterns consisting of broad halos, with indistinguishable second and third peaks

* Work supported by the U.S. Department of Energy, Office of Basic Energy Sciences, under Contract ER-78-S-02-4899.
** Present address: Kulicke & Soffa Industries, Inc., 507 Prudential Road, Horsham, PA 19044, USA.

corresponding to the {220} and {311} Bragg reflections (Kamins [2], Emmanuel and Pollock [3], Schwidefsky [4], Anderson [5], Kamins and Cass [6], Kühl et al. [7], and Nagasima and Kubota [8]).

The noncrystalline–crystalline transition of CVD silicon films occurs at a deposition temperature of 675°C (Anderson [5]). Above this temperature the CVD films consist of grains, the dimensions of which increase with the deposition temperature. In some cases, sharp, distinct diffraction peaks have been observed on samples prepared at lower temperatures (Kamins and Cass [6], Seto [9]). Doping by boron reduces this transition temperature to 500°C (Hall et al. [10], Cowher and Sedgwick [11]). Amorphous CVD silicon films, prepared at 620°C, have been reported to crystallize at a temperature of 665°C by differential thermal analysis measurements (Nagasima and Kubota [8b]). An abrupt change of the refractive index, also indicating the amorphous-to-crystalline transition, has been reported at 680°C (Hirose et al. [12]). The narrow range of crystallization temperatures of amorphous CVD silicon films which has been reported is interesting in view of the fact that other preparation methods produce samples that crystallize over a wide range of temperatures between 450°C and 825°C (Brodsky [13], Brodsky et al. [14], Moss and Graczyk [15], Lewis [16], Blum and Feldman [17], Mountvala and Abowitz [18], Tsai et al. [19], and Ackley and Tauc [20]). It should be kept in mind, however, that the crystallization of amorphous silicon below its melting point is a spontaneous process, so it is not just temperature- but also time-dependent. Thus the phrase "temperature of crystallization" actually should not be used without specifying the annealing time and the stage of annealing at which the sample is considered to be crystallized.

In the present investigation we were mainly interested in the kinetics of the crystallization process. We report the results of the measurements of the optical reflectance, the optical transmittance, the X-ray diffraction and the film thickness of CVD amorphous silicon as a function of annealing time. Effects of stress that were observed during annealing are reported. The results of this investigation show that CVD silicon films prepared between 550 and 660°C are in the anneal-stable amorphous state. The volume contraction upon crystallization agrees with the prediction of the continuous random network model (Turnbull and Polk [21], Polk [22], and Brodsky et al. [23]).

The results reported here are significant for the development of photothermal solar energy converters that use silicon as the absorbing element. As has been pointed out since 1974, the spectral inadequacy of a silicon absorber would be improved if the material could be used in its amorphous rather than in its polycrystalline form (Seraphin [24a, b], Griffith [25]). Since the shape and spectral location of the absorption edge of amorphous silicon vary widely with the conditions of preparation, the possibility exists of "tailoring" the absorption profile to give a performance superior to that of the crystalline material. In the amorphous material, a density-of-state profile that extends into the energy gap and a weakening of the requirements for momentum conservation both provide additional absorption strength in the visible and the near infrared. The same additional states localize free carriers and render the amorphous phase more transparent in the infrared than the crystalline form, thus suppressing the thermal emittance at high temperatures. Low crystallization temperatures of amorphous silicon which were reported in the literature have discouraged the utilization of these optical advantages, however. The fact that amorphous silicon films fabricated by CVD are stable at the anticipated operation temperature of photothermal converters is of technological consequence. It opens the possibility of manufacturing silicon absorbers with a performance superior to that of polycrystalline films and utilizing CVD as a method with established economical large-scale potential (Seraphin [24b, c]).

2. Experimental

2.1. Sample preparation

Silicon films of thicknesses ranging from 0.5 to 4 μm were deposited by pyrolytic decomposition of silane on fused silica substrates in a horizontal, radiation-heated reactor (Applied Materials Model AMH 704). A helium carrier gas flow of 10 l/min was maintained, and silane concentrations of 0.25% and 1% were used. Deposition temperatures ranged from 550 to 800°C and were determined with an accuracy of $\pm$5°C. Deposition rates ranged from 1.5 to 35 Å/s, depending on silane concentration and temperature. The deposition rate was monitored in situ by an infrared interference method (Kamins and Delloca [26]). About 50 samples, prepared in separate runs, were used in this investigation.

2.2. Annealing procedure

Samples were annealed in a flowing helium atmosphere. The annealing temperature was monitored to $\pm$1°C. Each sample was annealed at a constant temperature for several successive periods of time. Before and after each anneal, the optical transmittance, reflectance, X-ray diffraction pattern, and film thickness were measured at room conditions. Samples that were returned to the furnace regained their annealing temperature in less than 5 min with no temperature overshoot. The annealing times were measured from the moment the sample was inserted into the furnace.

2.3. Thickness measurements

The thickness of the films was measured with a Mirau two-beam interference objective (Leitz Wetzlar), after etching a step in the silicon film. This method does not require the step to be coated with a high-reflection film, which might affect the annealing behavior of the sample (Chang et al. [27]). The interferograms were recorded with both white and monochromatic (5460 Å) illumination, enlarged and analyzed. By this technique, thickness changes were detected with a resolution of $\pm$100 Å, and the absolute thickness was measured with an accuracy of $\pm$200 Å. Most results reported below refer to films of thicknesses ranging from 1.5 to 2 μm.

2.4. Optical measurements

The refractive index of the films was calculated from the spectral positions of the minima of the interference fringes of the reflected light. The reflectance was measured with a Perkin–Elmer double-beam spectrophotometer model 137 ($2.5\ \mu m \leqslant \lambda \leqslant 15\ \mu m$) and model 450 ($0.5\ \mu m \leqslant \lambda \leqslant 2.7\ \mu m$). The refractive index was determined in the wavelength region in which the absorption coefficient is less than 3×10^4 cm^{-1}, so the contribution of the imaginary part of the refractive index is negligible. The value of the refractive index was determined with an accuracy of $\pm 1.5\%$, limited by the accuracy of the determination of the sample thickness. However, by placing the samples in the spectrophotometer at the same position after each anneal, refractive index variations could be detected with a resolution of $\pm 0.5\%$ for a given sample $\approx 1.8\ \mu m$ thick.

The absorption coefficient α was calculated from the transmittance T according to (Connell et al. [28])

$$T=\frac{(1-R_1)(1-R_2)(1-R_3)e^{-\alpha d}}{1-R_2R_3+(2R_1R_2R_3-R_1R_2-R_1R_3)e^{-2\alpha d}}, \quad (1)$$

where R_1, R_2 and R_3 are the reflectances of the air–film, film–substrate, and substrate–air interfaces, respectively, and d is the film thickness. In the near infrared the interference fringes were averaged by taking into account the values of the transmittance at wavelengths that correspond to the mean values of the wavenumbers of two adjacent maxima and minima only. Values of α were determined only for $\alpha \geqslant 1000$ cm^{-1}. At lower absorptances the accuracy of the results was limited either due to scattering, which affects the results of some samples, or due to the limited accuracy of the determination of the value of R_1 in eq.(1). R_1 was calculated from

$$R_1=[(n-1)/(n+1)]^2, \quad (2)$$

where n is the refractive index of the silicon film as obtained from the interference fringe method. However, as pointed out in the literature, the refractive index that is obtained from the interference fringe method may be different from the surface refractive index (Schwidefsky [4], Kühl et al. [7]). Besides, since the analysis of our samples, and particularly the cooling from the annealing temperature down to room temperature, was done at room atmosphere, a thin oxide layer was formed on the sample surface, thus affecting the sample reflectance. This oxide layer was very thin, and unless otherwise specified it did not affect the reported results. In calculating R_2 and R_3 we used the value 1.45 for the refractive index of the substrate.

2.5. Structure characterization

The structure of the films was determined by a GE XRD-5 X-ray diffractometer, using a Cu target and a Ni filter ($\lambda=1.54$ Å). The angular resolution of the detector was 0.2°.

3. Experimental results

3.1. Effects of deposition temperature

Fig. 1 shows the absorption coefficient of six samples prepared at substrate temperatures T_s between 550 and 780°C. Within the experimental error, samples prepared below 650°C have the same profiles of absorption coefficient. Profiles of samples prepared at 685°C are intermediate to the 650°C and 750°C profiles. Samples prepared above 750°C again resemble each other in their absorption coefficient profiles.

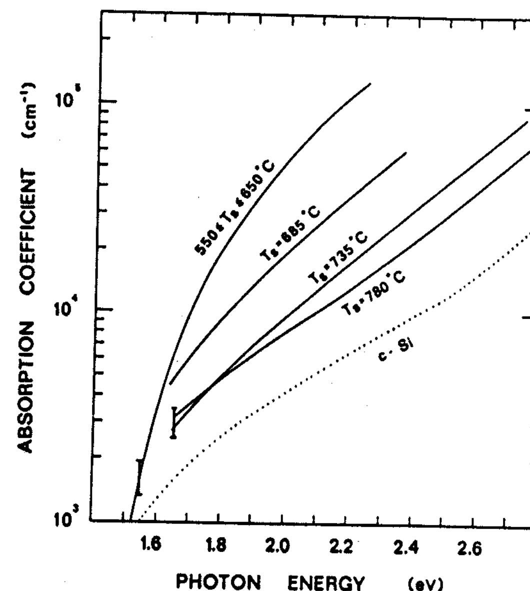

Fig. 1. The absorption coefficients of samples of various deposition temperatures T_s and thicknesses d(T_s=550, 590, 635, 685, 735, 780°C; d=0.58, 1.79, 1.67, 1.66, 0.85, 0.80 μm, respectively). The first three samples have the same absorption profile. The absorption profile of silicon single crystal (c-Si) is from Dash and Newman [48].

The X-ray diffraction patterns of the films prepared below 650°C are indicative of an amorphous structure. The average diameter of the coherently scattering regions, as obtained from the angular width of the {111} diffraction (Cullity [29]), is (19 ± 2) Å. For $T_s \approx 670$°C, small and relatively broad peaks appear. These peaks narrow and their intensity increases gradually as the deposition temperature increases. At $T_s=685$°C the average particle size is (70 ± 20) Å, and it reaches ≈ 200 Å at $T_s=715$°C. In the range $670°C \leqslant T_s \leqslant 750°C$ our peak-height results follow qualitatively the results reported by Kamins and Delloca [26], though there appears a large amount of scatter of the peak height ratios $I\{111\}/I\{220\}$. No anomaly of the kind they report for the range $600°C \leqslant T_s \leqslant 650°C$ was observed in our samples.

For films deposited in the range $670°C \leq T_s \leq 750°C$ the film's surface is usually rough and scatters light severely. Films deposited below this temperature range are rather smooth. The surface scattering increases with thickness. In the samples that were prepared above $T_s = 670°C$ we found cracks of the kind described by Mountvala and Abowitz [18]. For depositions below that range, the films were free of cracks.

3.2. Effects of annealing

Fig. 2 shows the absorption coefficient, and fig. 3 shows the refractive index of sample #20 ($T_s = 590°C$, $d = 1.79$ μm) as deposited and after annealing at 650°C for 75 min, 105 min, 130 min, 265 min, and after two further anneals at 850°C and 1030°C for 1 h each. As can be seen, after 75 min of annealing, both the absorption coefficient and the refractive index still coincide with the as-deposited profiles,

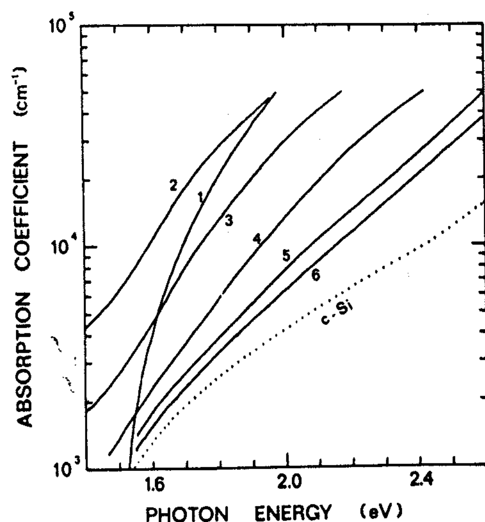

Fig. 2. The absorption coefficient of sample #20 ($T_s = 590$ C, $d = 1.79$ μm) after various annealing periods: 1. As deposited and after 75 min at $T_a = 650°C$. 2. After 105 min at $T_a = 650°C$. 3. After 130 min at $T_a =$ 650 C. 4. After 265 min at $T_a = 650°C$. 5. After another 60 min at $T_a = 850°C$. 6. After another 60 min at $T_a = 1030°C$. Curve for c-Si is from Dash and Newman [48].

indicating that no measurable change has occurred. After further annealing, the absorption of the film at the absorption edge increases, shifts to lower energies, and changes in slope. After further annealing, the absorption profile shifts back to higher energies and approaches that of single-crystal silicon. The value of the refractive index decreases monotonically in the near infrared, and its profile shifts to higher energies.

Fig. 4 shows the peak intensity of the X-ray {111} diffraction, $I\{111\}$, the photon energy corresponding to an absorption value of $\alpha = 10^4$ cm^{-1}, E_0, and the refractive index at a photon energy 0.5 eV, n_{IR}, all values observed on sample #20 as a function of annealing time at 650°C. Also shown in the figure are the corresponding values

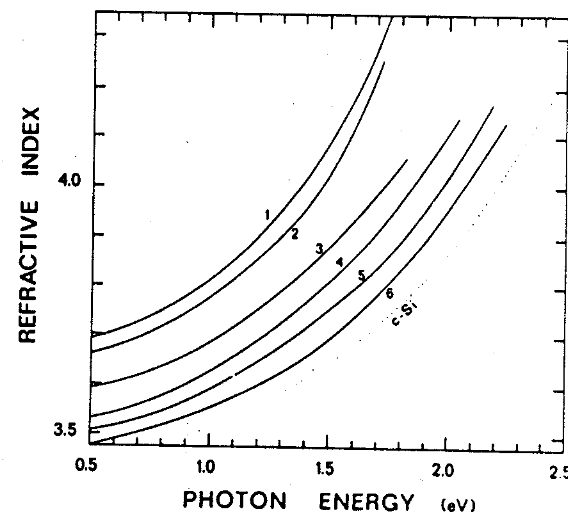

Fig. 3. The refractive index vs. photon energy after various annealing periods (same sample and annealing conditions as in fig. 2). The silicon single crystal data are taken from Philipp and Taft [49] and Salzberg and Villa [50].

after successive anneals at 850°C and at 1030°C, each for 1 h, and the asymptotic values of E_0 and n_{IR} of single-crystal silicon. As seen from the figure, the X-ray diffracted intensity, the absorption coefficient, and the refractive index of the film remain unchanged for about 75 min. After that time all three variables change simultaneously; the X-ray peak and the infrared refractive index change monotonically, while the absorption edge first shifts to lower energies and then shifts back to higher energies, approaching the crystalline value. The time dependence of the thickness showed a gradual decrease coincident with the increase of the {111} peak height in the diffraction pattern. The total decrease of thickness is $(1.5 \pm 1)\%$. For other annealing temperatures we obtained curves similar to those of fig. 4, with only a different time scale.

After the seventh anneal (105 min annealing), cracks appeared in sample #20. The number of cracks increased with further annealing. Similar cracks appeared in each annealed sample as soon as the X-ray diffraction peak reached approximately one-third of its saturation value. Since no damage was observed in amorphous films whose temperature cycling did not involve phase transformation, we concluded that the stress associated with the volume contraction during crystallization is much larger than the stress due to the mismatch of the thermal expansion coefficients of the silicon film and the silica substrate. Fig. 5a is a microinterferogram of the surface of a cracked sample. As can be seen from the photograph, the cracks are sharp lines that separate the sample into grains of ≈100 μm in diameter. Fig. 5b is a schematic diagram of the cross section of a crack in the sample. The peak-shaped grain boundaries are ≈400 Å above the surface of the sample. After the 850 C anneal, a few grains curved and flaked off the sample. These flakes consisted of the 1.8 μm

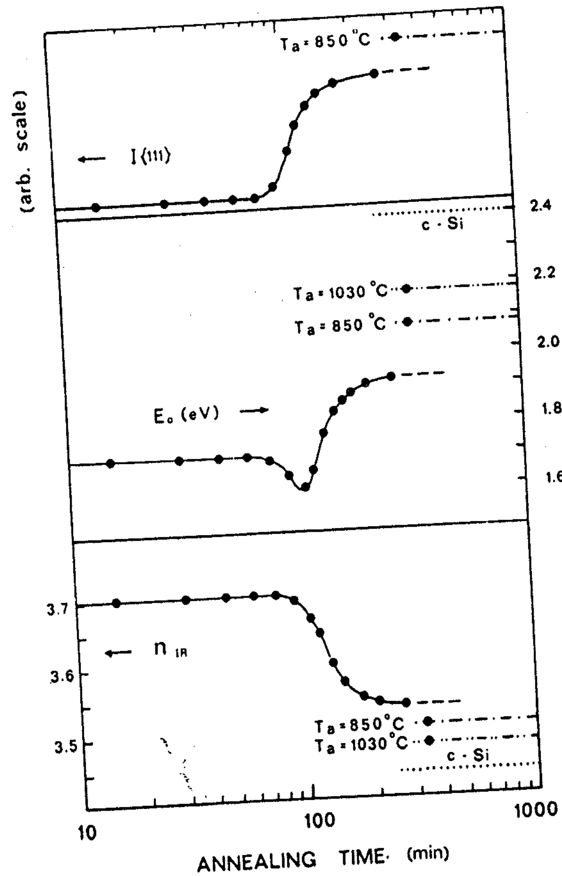

Fig. 4. The intensity of the {111} peak of the X-ray diffraction, $I\{111\}$, the photon energy corresponding to an absorption $\alpha = 10^4\ cm^{-1}$, E_0, and the refractive index at $h\nu = 0.5$ eV, n_{IR}, as a function of annealing time at 650°C. Also shown are the corresponding values after two further anneals at 850 and 1030°C, for 1 h each, and the crystalline values of E_0 and n_{IR}.

silicon film plus about a 10 μm thick silica layer that was split off the substrate. These flakes indicate that the adherence of the CVD silicon film to the fused silica substrate is at least as strong as the internal bonding force of the fused silica itself.

4. Discussion of experimental results

4.1. Properties of CVD amorphous silicon

Amorphous silicon films may undergo two kinds of thermally induced transformations. The first kind of transformations, which were thoroughly investigated in the past, are transformations between various degrees of amorphicity. In that region of

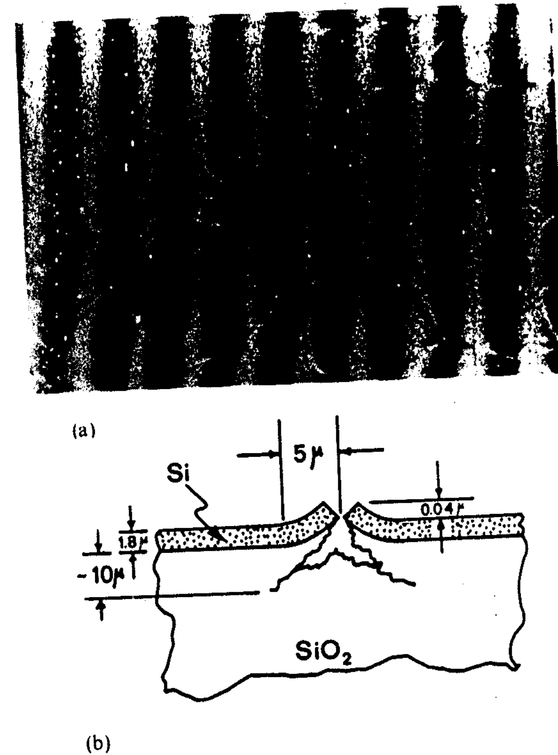

Fig. 5. (a) Crystallized silicon film on a fused silica substrate. The photograph was taken through a double beam interference objective with $\lambda = 546$ nm (×100 magnification). (b) A schematic diagram of the cross section of the above sample in the vicinity of a crack.

transformations the tensile stress (Koos and Neumann [30]), the ESR signal (Brodsky et al. [14], LeComber et al. [31]), the number of voids (Moss and Graczyk [15], Lewis [32]), the infrared refractive index (Brodsky et al. [14]), the absorption at the optical edge (Brodsky et al. [14], Brodsky and Gambino [33], Lewis [16], LeComber et al. [31]), and the electrical conductivity (Brodsky et al. [14], Lewis [16], LeComber et al. [31]) all decrease with annealing. A similar behavior of these parameters was reported on amorphous germanium (Connell et al. [28], Paesler [34], Theye et al. [35]). (If the sample is hydrogenated, the hydrogen effusion may interfere with some of these phenomena (Tsai et al. [19], Knights [36]).) Most of the reports suggest that in both amorphous silicon and germanium these transformations come to a completion after the sample is annealed for several hours at (or prepared at) about 100°C below the "temperature of crystallization", that is, at about 300°C for germanium and 500°C for silicon. At that stage an anneal-stable state is reached (Lewis [16]), which is sometimes referred to as a "nearly ideal" amorphous state (Theye [1]). The second kind of transformation occurs when the amorphous material crystallizes. During the crystallization process, most of the above-mentioned parameters change in the same

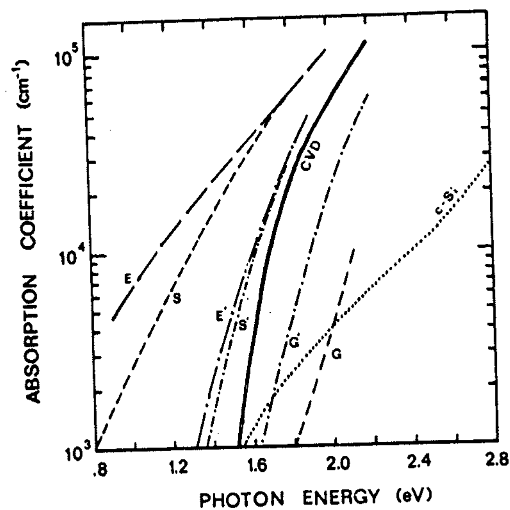

ig. 6. The absorption coefficient of amorphous silicon samples prepared by various methods, before and 'ter annealing: (E) Evaporated, as deposited ($T_s \approx 20°$C). (E') Evaporated, after annealing ($T_a = 377$°C). i) Sputtered, as deposited ($T_s = 20$°C). (S') Sputtered, after annealing ($T_a = 400$°C). (G) Glow discharge :composition of silane, as deposited ($T_s = 20$°C). (G') Glow discharge, as deposited ($T_s \simeq 300$°C). (CVD) 'his work (550°C $\leq T_s \leq$ 650°C). References: E and E', LeComber et al. [31], S and S', Brodsky et al. [14], G and G', Loveland et al. [37], c-Si, Dash and Newman [48].

nanner as they do during the transformations between the various amorphous stages; ıowever, the anneal-stable region separates between the two annealing processes. Our work deals with the second kind of transformation. The fact that in our experi- nents all the samples that were prepared below the onset of crystallization have the same absorption profile, and that annealing does not change the optical or structural properties of our films until crystallization starts, indicates that our films are in the anneal-stable amorphous state.

Fig. 6 shows the absorption profiles of evaporated, sputtered and glow discharge amorphous silicon films as deposited at room temperature and after being annealed at elevated temperatures. (For glow-discharge amorphous silicon we show the absorption profile of a sample prepared at $T_s = 300$°C rather than that of an annealed sample; however, the effect of increased deposition temperature on the absorption profile is similar to the effect of annealing (Theye [1]).) Also shown in fig. 6 are our CVD amorphous silicon results. As can be seen, while absorption profiles of annealed, sputtered and evaporated samples approach our results from the left (Brodsky et al. [14], Lewis [16], LeComber et al. [31]), the glow-discharge results approach our results from the right (Knights [36], Loveland et al. [37]). For anneal-stable amorphous silicon, the asymptotic value of the optical gap, E_{0e}, as extrapolated from the relation $\sqrt{\alpha h\nu} \propto (h\nu - E_{0e})$, is 1.6 eV, independent of the origin and the history of the film (Theye [1], Fritzsche [38]). The meaning of this extrapolation is controversial, but it is, however, a convenient method of comparing results of different sources. Fig. 7 is a plot of $\sqrt{\alpha h\nu}$ vs. photon energy for our CVD amorphous

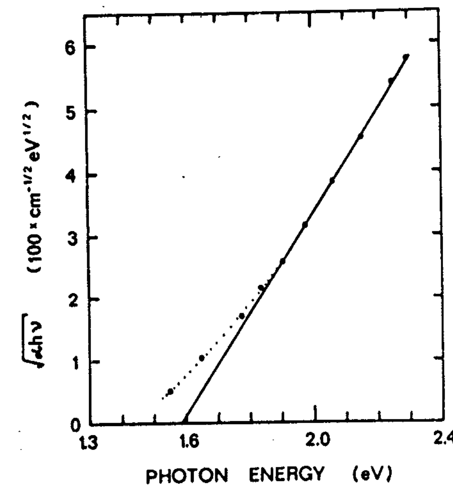

Fig. 7. $\sqrt{\alpha h\nu}$ vs. $h\nu$ for CVD amorphous silicon (dotted line) and the extrapolation to $\alpha = 0$ (solid line): 550°C $\leq T_s \leq$ 650 C.

silicon films, from which we extrapolate $E_{0e} = (1.59 \pm 0.02)$ eV. Reproducibility tests on four different samples prepared at $T_s = 550$, 580, 590 and 635°C, and with thicknesses of 0.58, 2.12, 1.79 and 1.67 μm respectively give the same results within the limit of the experimental error. Hirose et al. [12] reported a value of $E_{0e} = 1.45$ eV for CVD amorphous silicon. Their absorption profiles for both the amorphous and polycrystalline films in the range $1.5 \times 10^3 \leq \alpha \leq 2 \times 10^4$ cm^{-1} are identical to our results, however. Unfortunately, they do not report the absorption data at $\alpha \geq 5 \times 10^4$ cm^{-1}, which is essential for the extrapolation (Theye [1]).

The average size of the coherently scattering regions of our amorphous films, (19 ± 2) Å, agrees with the results of others (Brodsky [13], Brodsky et al. [14]). The extrapolation of the value of the infrared refractive index of our amorphous samples to zero energy gives 3.67 ± 0.05, which agrees with the value given by Schwidefsky [4] for the same size of coherently scattering particles. The correlation between our optical measurements and the results given by others (Schwidefsky [4], Kühl et al. [7], Hirose et al. [12]) shows that, independent of the details of preparation, all CVD amorphous silicon samples, prepared between 550 and 660°C, have essentially the same properties. The nature of the carrier gas in the CVD reactor may affect the absorption at values below 10^3 cm^{-1}, if at all.

The decrease in the thickness of our samples, (1.5 ± 1)%, combined with the excellent adherence of the silicon film to the fused silica substrate, suggests that the volume of the crystallized samples has decreased by (≈3 ± 2)%. This volume contraction is in agreement with the density deficiency of amorphous silicon according to the prediction of the continuous random network model (Turnbull and Polk [21], Polk [22], Brodsky et al. [23]).

Nagasima and Kubota [8b] reported a thickness decrease of 10% for their annealed

CVD amorphous silicon films. However, they do not report the experimental method that they employed for the thickness measurement. Sometimes the thickness is determined from the interference fringes obtained by an infrared spectrophotometer, assuming a constant refractive index. This may cause an error in the thickness change measurement, since the refractive index changes, too.

The deposition temperature at which we observe the first deviations from the typical amorphous X-ray diffraction, 670°C, is close to the 675°C reported by Anderson [5]. However, unlike his report on equiaxed, randomly oriented grains at higher deposition temperatures, we observe various preferred orientations of the kind reported by Kamins and Cass [6] and Nagasima and Kubota [8a].

4.2. Crystallization process of amorphous silicon

The kinetics of the crystallization is usually described by the Avrami formula (Christian [39], Turnbull and Cohen, [40])

$$x = 1 - \exp(-Bt^m), \tag{3}$$

where x is the fraction of the volume that has crystallized in time t after the beginning of crystallization, B is thermally activated, and $3 \leqslant m \leqslant 4$.

Let us assume that the X-ray diffracted intensity is proportional to the volume that has crystallized, that is,

$$I\{111\} = Ax(t) = A[1 - \exp(-Bt^m)], \tag{4}$$

where A is a proportionality constant. Fitting eq.(4) to our experimental results, we obtain the values $m=4$ and $B^{-1/m} = 115$ min at an annealing temperature T_a of 650°C. This fit can be improved if we shift the zero of the time scale to about 25 min after the beginning of the annealing. It is not clear whether this shift is meaningful in view of the experimental procedure that was employed (that is, nonnegligible periods of heating and cooling). At values of t satisfying $Bt^m \gg 1$, a better fit to the data is achieved by using $m \approx 3$, which can be interpreted as indicating the exhaustion of the crystallization nucleation centers (Christian [39]). The equation $Bt^m = 1$ is chosen as the criterion for the crystallization time of an amorphous sample.

The kinetics of the crystallization of amorphous silicon and germanium prepared by electron beam evaporation was investigated in the past by Blum and Feldman [17, 41]. The criterion that they used to indicate the crystallization is the drop in the value of the absorption coefficient of the annealed samples to 5×10^4 cm^{-1} at a wavelength of 4800 Å. This criterion should yield longer crystallization times than the criterion we gave above. Nevertheless, they reported a crystallization time of 105 min at $T_a = 650$°C, similar to our crystallization time at that temperature. The similarity of our and their results suggests that the thermally activated crystallization process of amorphous silicon on a fused silica substrate is independent of the method of preparation. Repeating our annealing experiments at $T_a = 550$°C and $T_a = 670$°C, we determined that in this temperature range the crystallization-time parameter B satisfies the equation

$$B^{1/4} = \nu_c \exp(-E_c/kT), \tag{5}$$

where $E_c = (3.4 \pm 0.2)$ eV and $\nu_c \simeq 5.3 \times 10^{14}$ s^{-1}, in agreement with Blum and Feldman [41].

If eq.(4) is used with time-independent values of A, B and m, we find that the asymptotic values of $I\{111\}$, E_0 and n_{IR} for $t \to \infty$ at $T_a = 650$°C are considerably lower than the values obtained after 1 h anneal at a higher temperature (see fig. 4). A possible explanation for this behavior is that eq.(3) correctly describes the process of crystallization only while crystals are growing at the expense of the amorphous phase. Once the individual crystalline grains have grown so that their boundaries touch each other, which is the case for $Bt^m \gg 1$, the kinetics laws are changed. The higher temperature annealings at 850 and 1030°C probably minimize the total area of the grain boundaries by growth of the grains at the expense of each other. At the lower temperatures this mechanism probably proceeds at a much slower rate than that given by eqs.(4) and (5).

Crystallization temperatures for amorphous silicon are frequently reported in the literature, usually without specifying the crystallization time or the crystallization criterion. Most of the results fall in the range (675 ± 25)°C, which according to eq.(5) gives crystallization times between 10 min and ≈ 2 h (Emmanuel and Pollock [3], Anderson [5], Nagasima and Kubota [8], Cowher and Sedgwick [11], Hirose et al. [12], Brodsky [13], Blum and Feldman [17], Mountvala and Abowitz [18], Tsai et al. [19]). In those cases where higher or lower crystallization temperatures are reported, extrinsic effects may have affected the crystallization process. For instance, experiments performed on germanium suggest that oxygen impurities increase the temperature of crystallization (Adamsky et al. [42], Adamsky [43]). Epitaxial growth tendencies on a crystalline substrate can also affect the crystallization temperature (Roth and Anderson [44]).

The shift of the values of the optical constants of the annealed samples toward lower values of α and n can be accounted for as a result of the superposition of two media having two different sets of optical constants – the amorphous and the crystalline (Baker [45]). This statement is supported by the resemblance of the time variation of the values of the optical constants and the fraction of the volume that has crystallized as indicated by the intensity of the X-ray diffraction. A detailed calculation will be given elsewhere. The values of the optical constants of samples deposited in the transition range ($670°\text{C} \leqslant T_s \leqslant 750°\text{C}$) may be explained in a similar way. We have, however, no experimental data on the relation between the values of the optical constants and the fraction of crystalline volume for samples prepared in this range.

4.3. The anomaly of the optical absorption

Despite many reports on a blue shift of the absorption edge upon crystallization, we observed that the crystallization of an annealed CVD amorphous silicon film on a fused silica substrate initially causes a red shift of the absorption edge. We offer two possible explanations for that anomaly. According to one explanation, the small crystalline islands that grow in the amorphous sea scatter the light within the bulk

of the material, due to the difference between the complex dielectric constants of the crystalline and amorphous regions. This scattering, which is an additional loss mechanism, appears as a red shift of the absorption. At the early stage of crystallization this volume-scattering is the dominant change, since the fraction of the volume that has crystallized is still too small to considerably affect the absorptance. After further annealing, as the volume fraction of crystalline silicon increases, the absorption edge shifts to the blue owing to the introduction of optical-transition selection rules and probable annihilation of optical active states near the band edges.

A second explanation of the anomaly of the absorption edge is associated with the stress that is developed in the film owing to the contraction upon crystallization. Connell and Paul [46] investigated the effect of pressure on the optical properties of amorphous silicon and have reported the values $dE_0/dP = 0.25$ meV/kbar and $(1/n)(dn/dP) = -5 \times 10^{-5}$ kbar^{-1}, where E_0 is the optical gap, n is the infrared refractive index, and P is the pressure. In our samples the silicon contraction, together with the perfect adherence of the silicon film to the silica substrate, creates a large tensile stress. According to the results of Connell and Paul, our observed red shift of about -0.1 eV can be explained by postulating a tensile stress of 4×10^{11} dyn/cm^2. This is an extraordinarily high stress, and indeed it results in the mechanical failure of the silicon film and the silica substrate. Again, after a large enough fraction of the volume has crystallized, the red shift is replaced by a blue shift.

The fact that the red shift anomaly is not revealed in the refractive index behavior speaks in favor of the first explanation. According to the results quoted above (Connell and Paul [46]), one would expect that a tensile stress of 4×10^{11} dyn/cm^2 would increase the value of the refractive index by about 2%, which is not observed in the experiments.

We do not think the red-shift anomaly is associated with hydrogen effusion, as was reported for hydrogenated glow-discharge amorphous silicon (Tsai et al. [19]), since the temperature range at which the red shift occurs due to hydrogen effusion is between 400 and 600°C and since the red shift due to hydrogen effusion is from a value of $E_{0e} \approx 1.9$ eV to a value of 1.7 eV, rather than from 1.6 to 1.5 eV, which we observe*.

4.4. Discussion of stresses

In fig. 5 we showed the cracks that developed during the continuing crystallization. Measurements of the profile of a few curved pieces that flaked from the substrate gave an estimation of a stress (Finegan and Hoffman [47]) on the order of 3×10^{10} dyn/cm^2, using the values 7.4×10^{11} dyn/cm^2 for the elastic (Young's) modulus and 0.16 for the Poisson ratio of the silica substrate**. This stress is an order of magnitude lower than the stress that was calculated above to explain the red shift of the absorption edge. However, a large uncertainty in the calculation of the stress from the profile of the cracks is introduced by the rough estimation of the thickness of the fused silica layer that adhered to the silicon and had been split from the substrate.

After annealing at 1030°C for 1 h, it was observed that many of the curved cracks straighten back, which can be interpreted as being due to an increased mobility of the atoms at that temperature, which enables effective diffusion of atoms or dislocations and relief of the strain. Some oxidation that occurred during these high temperature anneals may also be responsible for stress relief, as was observed in amorphous silicon (Koos and Neumann [30]) and germanium (Paesler [34]).

It seems that the thermal stress due to a mismatch of the silicon and silica expansion coefficients is small relative to the stress due to crystallization since repeated heating to 650°C without a structural change caused no cracks in the silicon-silica wafer. This is in agreement with the difference between the linear contraction of $\approx 1.5\%$ that is caused by crystallization, and the thermal contraction of only 0.18% when silicon is cooled from 650° to room temperature.

Koos and Neumann [30], who measured the stress in electron beam evaporated amorphous silicon, reported that above $T_s \approx 550$°C the slope of the plot of stress vs. annealing temperature decreases, and in fact only changes in thermal stress were observed above that temperature. They interpreted this decrease in slope as an indication of the beginning of the nucleation of crystalline silicon. We hypothesize that what they really observed was the reaching of the anneal-stable state, where all the internal stresses were relieved (Paesler [34]). Had they reached the beginning of crystallization, they would have observed a large and sudden increase in the tensile stress.

The fact that cracks are present in the polycrystalline samples but absent from the amorphous samples suggests that the stresses in amorphous CVD silicon films are relatively low. This mechanical stability of the CVD amorphous silicon film is significant for its practical use in a photothermal converter.

5. Conclusions

We have shown that CVD amorphous silicon has the properties of the anneal-stable amorphous material. The average dimension of its coherently scattering regions is (19 ± 2)Å, its extrapolated optical energy gap is (1.59 ± 0.02) eV, its infrared refractive index is 3.67 ± 0.05, and its density is $(97 \pm 2)\%$ of the crystalline density, in agreement with the random network model.

The thermally activated crystallization kinetics of CVD amorphous silicon generally follows the Avrami formula, and the crystallization time depends on the annealing temperature. It is suggested that the kinetics law of the crystallization process, together with extrinsic effects such as doping and the nature of the substrate, are responsible for the wide range of the temperatures of crystallization reported in the literature. The tensile stress that is developed during crystallization is large enough to crack both the silicon film and the fused silica substrate.

The absorption edge at the beginning of the crystallization shifts to the red instead of the blue, which is the general trend during the interamorphous and the amorphous–

* Recently, SIMS analysis has been performed on one of our CVD amorphous silicon films ($T_s = 600$°C) by Dr. C. W. Magee of RCA Laboratories, which showed it to contain 0.2% hydrogen. Glow-discharge amorphous hydrogenated silicon usually contains between 10 and 30 at% hydrogen.

** Corning Glass Works, 1971, Corning Fused Silica No. 7940 (Lem-FS 7940, GLD, USA).

crystalline transformations. This anomalous shift can be attributed either to the effect of stress or to the effect of volume scattering, when the first crystalline regions appear in the amorphous film. Only after further annealing is this red shift replaced by a net blue shift of the absorption profile, which eventually reaches the polycrystalline silicon absorption profile.

The results indicate the eventual feasibility of manufacturing amorphous silicon solar absorbers with a performance superior to that of polycrystalline films, utilizing CVD as a method with established economical large-scale potential. Since CVD amorphous silicon films are deposited in their anneal-stable state, no further transformation of their structure or their optical properties is expected during their operation as photothermal absorbers. It has been shown that CVD amorphous silicon films are at least as stable as amorphous silicon films prepared by other methods, despite their relatively high deposition temperature. The stabilizing effect of incorporated impurities seems promising and will be studied further.

Acknowledgements

The authors wish to thank Dr. H. Gurev, Dr. L. J. Demer and Mr. R. Shimshock for their help during various phases of the experiments; Dr. C. W. Magee for performing SIMS analysis; and Prof. P. S. Rudman for reading the manuscript and for his important remarks. In the course of this work we have significantly profited from stimulating discussions with Prof. G. Weiser during his sabbatical leave with our group.

M. Janai wishes to thank the AVIAC Foundation, Technion, Israel Institute of Technology, and the Fulbright–Hays Foundation for financial support.

References

[1] M. L. Theye, Structural Effects in the Optical Properties of Tetrahedrally Bonded Amorphous Semiconductors, in: Optical Properties of Solids – New Developments, ed. B. O. Seraphin (North-Holland, Amsterdam, 1976) ch. 7.
[2] T. I. Kamins, IEEE Trans. PHP 10 (1974) 221.
[3] A. Emmanuel and H. M. Pollock, J. Electrochem. Soc. 120 (1973) 1586.
[4] F. Schwidefsky, Thin Solid Films 18 (1973) 45.
[5] R. M. Anderson, J. Electrochem. Soc. 120 (1973) 1540.
[6] T. I. Kamins and T. R. Cass, Thin Solid Films 16 (1973) 147.
[7] C. Kühl, H. Schlötterer and F. Schwidefsky, J. Electrochem. Soc. 121 (1974) 1496.
[8] N. Nagasima and N. Kubota, (a) Jpn. J. Appl. Phys. 14(1975) 1105; (b) J. Vac. Sci. Technol. 14 (1977) 54.
[9] J. Y. W. Seto, J. Electrochem. Soc. 122 (1975) 701.
[10] L. H. Hall, K. M. Koliwad and L. M. Swink, Thin Solid Films 18 (1973) 145.
[11] M. E. Cowher and T. O. Sedgwick, J. Electrochem. Soc. 119 (1972) 1565.
[12] M. Hirose, M. Taniguchi and Y. Osaka, in: Amorphous and Liquid Semiconductors, ed. W. E. Spear (Center for Industrial Consultancy and Liaison, University of Edinburgh, 1977) p. 352.
[13] M. H. Brodsky, J. Vac. Sci. Technol. 8 (1971) 125.

[14] M. H. Brodsky, R. S. Title, K. Weiser and G. D. Pettit, Phys Rev. B 1 (1970) 2632
[15] S. C. Moss and J. F. Graczyk, Phys. Rev. Lett. 23 (1969) 1167.
[16] A. Lewis. Phys. Rev. Lett. 29 (1972) 1555.
[17] N. A. Blum and C. Feldman, J. Non-Cryst. Solids 11 (1972) 242.
[18] A. J. Mountvala and G. Abowitz, Vacuum 15 (1965) 359.
[19] C. C. Tsai, H. Fritzsche, M. H. Tanilian, P. J. Gaczi, P. D. Persans and M. A. Vesaghi, in: Amorphou and Liquid Semiconductors, ed. W. E. Spear (Center for Industrial Consultancy and Liaison, Un versity of Edinburgh, 1977) p. 339.
[20] D. E. Ackley and J. Tauc, Appl. Opt. 14 (1977) 2806.
[21] D. Turnbull and D. E. Polk, J. Non-Cryst. Solids 8–10 (1972) 19.
[22] D. E. Polk, J. Non-Cryst. Solids 5 (1971) 365.
[23] M. H. Brodsky, D. Kaplan and J. F. Ziegler, Appl. Phys. Lett. 21 (1972) 305.
[24] B. O. Seraphin (a) Proc. Symp. on Materials Sciences Aspects of Thin Film Systems in Solar Energ Conversion, Tucson, Ariz., 20–22 May 1974, NSF-RANN Grant No. GI-43-795 (1974) p. 7; (b) Japan Soc. Appl. Phys. 44 (1975) 11; (c) Thin Solid Films 39 (1976) 87.
[25] R. W. Griffith, Sharing the Sun – Solar Technology in the Seventies, Winnipeg, Canada, 15–20 Au 1975, Int. Solar Energy Soc., Vol. 6 (1976) p. 205; in: Amorphous and Liquid Semiconductor ed. W. E. Spear (Center for Industrial Consultancy and Liaison, University of Edinburgh, 1977) p. 45
[26] T. I. Kamins and D. J. Delloca, J. Electrochem. Soc. 119 (1972) 112.
[27] C. A. Chang, W. J. Siekhaus, T. Kaminska and D. T. C. Huo. Appl. Phys. Lett. 26 (1975) 178.
[28] G. A. N. Connell, W. Paul and R. J. Temkin, Adv. Phys. 22 (1973) 643.
[29] B. D. Cullity, Elements of X-ray Diffraction (Addison-Wesley, Reading, Mass., 1956).
[30] V. Koos and H. G. Neumann, Phys. Stat. Sol. (a) 36 (1976) K47.
[31] P. G. LeComber, R. J. Loveland, W. E. Spear and R. A. Vaughn, in: Amorphous and Liquid Sem conductors, eds. J. Stuke and W. Brenig (Taylor and Francis, London, 1974) p. 245.
[32] A. Lewis, Solid State Commun. 13 (1973) 547.
[33] M. H. Brodsky and R. J. Gambino, J. Non-Cryst. Solids 8–10 (1972) 739.
[34] M. Paesler, in: Amorphous and Liquid Semiconductors, eds. J. Stuke and W. Brenig (Taylor an Francis, London, 1974) p. 229.
[35] M. L. Theye, M. Gandais and S. Fisson, Phys. Stat. Sol. (a) 17 (1973) 643.
[36] J. C. Knights, in: Structure and Excitations of Amorphous Solids, eds. G. Lucovsky and F. I Galeener (AIP, 1976) p. 296.
[37] R. J. Loveland, W. E. Spear and A. Al Sharbaty, J. Non-Cryst. Solids 13 (1973–74) 55.
[38] H. Fritzsche, in: Amorphous and Liquid Semiconductors ed. W. E. Spear (Center for Industri Consultancy and Liaison, University of Edinburgh, 1977) p. 3.
[39] J. W. Christian, The Theory of Transformations in Metals and Alloys (Pergamon Press, New Yor 1965) Ch. 12.
[40] D. Turnbull and M. H. Cohen, in: Modern Aspects of the Vitreous State, ed. J. D. Mackenz (Butterworths, London, 1960) vol. 1, p. 38.
[41] N. A. Blum and C. Feldman, J. Non-Cryst. Solids 22 (1976) 29.
[42] R. F. Adamsky, K. H. Benndt and W. T. Brogan, J. Vac. Sci. Technol. 6 (1969) 542.
[43] R. F. Adamsky, J. Appl. Phys. 40 (1969) 4301.
[44] J. A. Roth and C. L. Anderson. Appl. Phys. Lett. 31 (1977) 689.
[45] A. S. Baker Jr., Phys. Rev. B 7 (1973) 2507.
[46] G. A. N. Connell and W. Paul, J. Non-Cryst. Solids 8–10 (1972) 215.
[47] J. D. Finegan and R. W. Hoffman, Trans. Eighth National Vacuum Symposium (Pergamon Pres New York, 1961) p. 935.
[48] W. C. Dash and R. Newman, Phys. Rev. 99 (1955) 1151.
[49] H. R. Philipp and E. A. Taft, Phys. Rev. 120 (1960) 37.
[50] C. Salzberg and J. Villa, J. Opt. Soc. Am. 47 (1957) 244.

crystalline transformations. This anomalous shift can be attributed either to the effect of stress or to the effect of volume scattering, when the first crystalline regions appear in the amorphous film. Only after further annealing is this red shift replaced by a net blue shift of the absorption profile, which eventually reaches the poly-crystalline silicon absorption profile.

The results indicate the eventual feasibility of manufacturing amorphous silicon solar absorbers with a performance superior to that of polycrystalline films, utilizing CVD as a method with established economical large-scale potential. Since CVD amorphous silicon films are deposited in their anneal-stable state, no further transformation of their structure or their optical properties is expected during their operation as photothermal absorbers. It has been shown that CVD amorphous silicon films are at least as stable as amorphous silicon films prepared by other methods, despite their relatively high deposition temperature. The stabilizing effect of incorporated impurities seems promising and will be studied further.

Acknowledgements

The authors wish to thank Dr. H. Gurev, Dr. L. J. Demer and Mr. R. Shimshock for their help during various phases of the experiments; Dr. C. W. Magee for performing SIMS analysis; and Prof. P. S. Rudman for reading the manuscript and for his important remarks. In the course of this work we have significantly profited from stimulating discussions with Prof. G. Weiser during his sabbatical leave with our group.

M. Janai wishes to thank the AVIAC Foundation, Technion, Israel Institute of Technology, and the Fulbright–Hays Foundation for financial support.

References

[1] M. L. Theye, Structural Effects in the Optical Properties of Tetrahedrally Bonded Amorphous Semiconductors, in: Optical Properties of Solids – New Developments, ed. B. O. Seraphin (North-Holland, Amsterdam, 1976) ch. 7.
[2] T. I. Kamins, IEEE Trans. PHP 10 (1974) 221.
[3] A. Emmanuel and H. M. Pollock, J. Electrochem. Soc. 120 (1973) 1586.
[4] F. Schwidefsky, Thin Solid Films 18 (1973) 45.
[5] R. M. Anderson, J. Electrochem. Soc. 120 (1973) 1540.
[6] T. I. Kamins and T. R. Cass, Thin Solid Films 16 (1973) 147.
[7] C. Kühl, H. Schlötterer and F. Schwidefsky, J. Electrochem. Soc. 121 (1974) 1496.
[8] N. Nagasima and N. Kubota, (a) Jpn. J. Appl. Phys. 14(1975) 1105; (b) J. Vac. Sci. Technol. 14 (1977) 54.
[9] J. Y. W. Seto, J. Electrochem. Soc. 122 (1975) 701.
[10] L. H. Hall, K. M. Koliwad and L. M. Swink, Thin Solid Films 18 (1973) 145.
[11] M. E. Cowher and T. O. Sedgwick, J. Electrochem. Soc. 119 (1972) 1565.
[12] M. Hirose, M. Taniguchi and Y. Osaka, in: Amorphous and Liquid Semiconductors, ed. W. E. Spear (Center for Industrial Consultancy and Liaison, University of Edinburgh, 1977) p. 352.
[13] M. H. Brodsky, J. Vac. Sci. Technol. 8 (1971) 125.

[14] M. H. Brodsky, R. S. Title, K. Weiser and G. D. Pettit, Phys Rev. B 1 (1970) 2632
[15] S. C. Moss and J. F. Graczyk, Phys. Rev. Lett. 23 (1969) 1167.
[16] A. Lewis, Phys. Rev. Lett. 29 (1972) 1555.
[17] N. A. Blum and C. Feldman, J. Non-Cryst. Solids 11 (1972) 242.
[18] A. J. Mountvala and G. Abowitz, Vacuum 15 (1965) 359.
[19] C. C. Tsai, H. Fritzsche, M. H. Tanilian, P. J. Gaczi, P. D. Persans and M. A. Vesaghi, in: Amorphous and Liquid Semiconductors, ed. W. E. Spear (Center for Industrial Consultancy and Liaison, University of Edinburgh, 1977) p. 339.
[20] D. E. Ackley and J. Tauc, Appl. Opt. 14 (1977) 2806.
[21] D. Turnbull and D. E. Polk, J. Non-Cryst. Solids 8–10 (1972) 19.
[22] D. E. Polk, J. Non-Cryst. Solids 5 (1971) 365.
[23] M. H. Brodsky, D. Kaplan and J. F. Ziegler, Appl. Phys. Lett. 21 (1972) 305.
[24] B. O. Seraphin (a) Proc. Symp. on Materials Sciences Aspects of Thin Film Systems in Solar Energy Conversion, Tucson, Ariz., 20–22 May 1974, NSF-RANN Grant No. GI-43-795 (1974) p. 7; (b) J. Japan Soc. Appl. Phys. 44 (1975) 11; (c) Thin Solid Films 39 (1976) 87.
[25] R. W. Griffith, Sharing the Sun – Solar Technology in the Seventies, Winnipeg, Canada, 15–20 Aug. 1975, Int. Solar Energy Soc., Vol. 6 (1976) p. 205; in: Amorphous and Liquid Semiconductors, ed. W. E. Spear (Center for Industrial Consultancy and Liaison, University of Edinburgh, 1977) p. 457.
[26] T. I. Kamins and D. J. Delloca, J. Electrochem. Soc. 119 (1972) 112.
[27] C. A. Chang, W. J. Siekhaus, T. Kaminska and D. T. C. Huo, Appl. Phys. Lett. 26 (1975) 178.
[28] G. A. N. Connell, W. Paul and R. J. Temkin, Adv. Phys. 22 (1973) 643.
[29] B. D. Cullity, Elements of X-ray Diffraction (Addison-Wesley, Reading, Mass., 1956).
[30] V. Koos and H. G. Neumann, Phys. Stat. Sol. (a) 36 (1976) K47.
[31] P. G. LeComber, R. J. Loveland, W. E. Spear and R. A. Vaughn, in: Amorphous and Liquid Semiconductors, eds. J. Stuke and W. Brenig (Taylor and Francis, London, 1974) p. 245.
[32] A. Lewis, Solid State Commun. 13 (1973) 547.
[33] M. H. Brodsky and R. J. Gambino, J. Non-Cryst. Solids 8–10 (1972) 739.
[34] M. Paesler, in: Amorphous and Liquid Semiconductors, eds. J. Stuke and W. Brenig (Taylor and Francis, London, 1974) p. 229.
[35] M. L. Theye, M. Gandais and S. Fisson, Phys. Stat. Sol. (a) 17 (1973) 643.
[36] J. C. Knights, in: Structure and Excitations of Amorphous Solids, eds. G. Lucovsky and F. L. Galeener (AIP, 1976) p. 296.
[37] R. J. Loveland, W. E. Spear and A. Al Sharbaty, J. Non-Cryst. Solids 13 (1973–74) 55.
[38] H. Fritzsche, in: Amorphous and Liquid Semiconductors ed. W. E. Spear (Center for Industrial Consultancy and Liaison, University of Edinburgh, 1977) p. 3.
[39] J. W. Christian, The Theory of Transformations in Metals and Alloys (Pergamon Press, New York, 1965) Ch. 12.
[40] D. Turnbull and M. H. Cohen, in: Modern Aspects of the Vitreous State, ed. J. D. Mackenzie (Butterworths, London, 1960) vol. 1, p. 38.
[41] N. A. Blum and C. Feldman, J. Non-Cryst. Solids 22 (1976) 29.
[42] R. F. Adamsky, K. H. Benndt and W. T. Brogan, J. Vac. Sci. Technol. 6 (1969) 542.
[43] R. F. Adamsky, J. Appl. Phys. 40 (1969) 4301.
[44] J. A. Roth and C. L. Anderson, Appl. Phys. Lett. 31 (1977) 689.
[45] A. S. Baker Jr., Phys. Rev. B 7 (1973) 2507.
[46] G. A. N. Connell and W. Paul, J. Non-Cryst. Solids 8–10 (1972) 215.
[47] J. D. Finegan and R. W. Hoffman, Trans. Eighth National Vacuum Symposium (Pergamon Press, New York, 1961) p. 935.
[48] W. C. Dash and R. Newman, Phys. Rev. 99 (1955) 1151.
[49] H. R. Philipp and E. A. Taft, Phys. Rev. 120 (1960) 37.
[50] C. Salzberg and J. Villa, J. Opt. Soc. Am. 47 (1957) 244.